Effects of large salinity fluctuations on an anaerobic membrane bioreactor treating phenolic wastewater

Muñoz Sierra, Julian D.; Oosterkamp, Margreet J.; Spanjers, Henri; van Lier, Jules B.

DOI
10.1016/j.cej.2021.129263

Publication date
2021

Document Version
Final published version

Published in
Chemical Engineering Journal

Chemical Engineering Journal 417 (2021) 129263

Contents lists available at ScienceDirect

Chemical Engineering Journal

journal homepage: www.elsevier.com/locate/cej

Effects of large salinity fluctuations on an anaerobic membrane bioreactor treating phenolic wastewater

Julian D. Muñoz Sierra [a,b,*], Margreet J. Oosterkamp [a,c], Henri Spanjers [a], Jules B. van Lier [a]

[a] Section Sanitary Engineering, Department of Water Management, Delft University of Technology, Stevinweg 1, 2628CN Delft, the Netherlands
[b] KWR Water Research Institute, Groningenhaven 7, 3430 BB Nieuwegein, the Netherlands
[c] Environmental Technology, Wageningen University & Research, Bornse Weilanden 9, 6708WG Wageningen, the Netherlands

ARTICLE INFO

Keywords:
AnMBR
Biomass characteristics
Phenol
Microbial diversity
Salinity fluctuations

ABSTRACT

High salinity is becoming more common in industrial process water and final effluents, particularly when striving to close water loops. There is limited knowledge on the anaerobic treatment of chemical wastewaters characterized by distinct salinity fluctuations. This study investigates the high and fluctuating salinity effects on the conversion capacity and membrane filtration performance of an anaerobic membrane bioreactor (AnMBR) in treating phenol-containing wastewater. The AnMBR operated for 180 days with sodium concentrations between 8 and 37 $gNa^{+}{\cdot}L^{-1}$. At $\leq$ 26 $gNa^{+}{\cdot}L^{-1}$, approximately 99% COD and phenol removal efficiencies were achieved. At 37 $gNa^{+}{\cdot}L^{-1}$, phenol and COD removal efficiencies decreased to 86 and 82%, respectively, while the biomass specific methanogenic activity was 0.12 ± 0.05 $gCOD\text{-}CH_4{\cdot}gVSS^{-1}{\cdot}d^{-1}$. Due to large salinity fluctuations, phenol and COD removal efficiencies reduced to $\leq$ 45% but recovered to $\geq$ 88%. Compared to phenol conversion, methanogenesis was more severely affected. Calculations showed a maximum in-situ phenol conversion rate of 25.5 $mgPh{\cdot}gVSS^{-1}{\cdot}d^{-1}$. Concomitantly, biomass integrity was compromised, and the median particle size severely dropped from 65.6 to 4.3 μm, resulting in a transmembrane pressure increase above 400 mbar. Cake layer resistance to filtration contributed to 85% of the total resistance. Nonetheless, all biomass was effectively retained in the AnMBR. A change in salinity $\geq$ 14 $gNa^{+}{\cdot}L^{-1}$ substantially reduced the microbial richness and diversity. The microbial community was dominated by Bacteria belonging to Clostridiales and Archaea of the orders Methanosarcinales and Methanobacteriales. Our findings demonstrate AnMBRs as suitable techniques for treating chemical process water, with possible subsequent reclamation, characterized by high phenols concentrations and largely fluctuating salinity levels.

1. Introduction

Worldwide, the introduction of cleaner industrial production processes has promoted closing water cycles, particularly in water-intensive industries, such as the chemical industry [1]. Consequently, industrial residual waters are becoming increasingly associated with extreme conditions, such as high salinity and the presence of high concentrations of toxic aromatic compounds that can adversely reduce biological activity [2]. Inorganic salts in wastewaters are mainly present as sodium chloride (NaCl). Moreover, hypersaline wastewater streams represent 5% of the world's total industrial effluents [3]. High sodium concentrations may reduce the effectiveness of anaerobic treatment and could induce the disintegration of flocs or granules, leading to operational challenges [4], although anaerobic consortia may adapt to high salinity levels [5].

Previous studies have reported the effect of increasing sodium concentrations on high-rate anaerobic reactors for both granular sludge bed and membrane-based systems. Vyrides and Stuckey [6] reported that anaerobic biomass could acclimate to sodium concentrations from 4 to 12 $gNa^{+}{\cdot}L^{-1}$. Ismail et al. [7] suggested that by increasing sodium concentration from 5 to 20 $gNa^{+}{\cdot}L^{-1}$ in a UASB, sludge granulation was hampered following a considerable reduction in granule strength by the exchange of calcium with sodium ions. However, when adding calcium to the influent to compensate exchange losses, Sudmalis et al. [8] noted stable granule formation at both 5 and 20 $gNa^{+}{\cdot}L^{-1}$ concentration in a UASB reactor, although the COD removal efficiency was reduced at 20 $gNa^{+}{\cdot}L^{-1}$. Song et al. [9] concluded that in an AnMBR, a step-wise increase in the sodium concentration beyond 4 $gNa^{+}{\cdot}L^{-1}$ reduced the COD

* Corresponding author.
E-mail addresses: J.D.MunozSierra@tudelft.nl, julian.munoz@kwrwater.nl (J.D. Muñoz Sierra).

https://doi.org/10.1016/j.cej.2021.129263
Received 29 November 2020; Received in revised form 27 February 2021; Accepted 2 March 2021
Available online 10 March 2021

removal efficiency to values lower than 80%. Similarly, Chen et al. [10] demonstrated a decrease in the COD removal efficiency from 96% to 78% by sequentially increasing the sodium concentration from 0 to 2, 4, 8, and 16 $gNa^{+}{\cdot}L^{-1}$. In contrast, in our previous study, we achieved COD removal efficiencies exceeding 90% in an AnMBR treating phenol-containing wastewater, after a step-wise increase in the sodium concentration from 8 to 18 $gNa^{+}{\cdot}L^{-1}$ [11]. Furthermore, in a comparative study, we showed the superiority of an AnMBR over a UASB reactor following a step-wise increase in sodium concentration from 16 to 26 $gNa^{+}{\cdot}L^{-1}$ [12]. The long-term calcium wash-out led to a disintegration of granules and failure of the UASB at 26 $gNa^{+}{\cdot}L^{-1}$. It should be realized that large amounts of industrial effluents containing priority organic pollutants, such as phenol, exhibit very high salt concentrations. Sodium chloride in phenolic wastewaters from chemical processes and agro-food industries ranged from 2 to 100 $gNaCl{\cdot}L^{-1}$ [13,14] which is equivalent to approximately 0.8 to 39 $gNa^{+}{\cdot}L^{-1}$.

Regarding the microbial community composition, Lu et al. [15] showed that a salinity increase from 0 to 9.2 $gNa^{+}{\cdot}L^{-1}$ only enriched specific lineages, but no drastic changes in the composition were observed. In contrast, Chen et al. [10] indicated that a step-wise salinity increase to about 16 $gNa^{+}{\cdot}L^{-1}$ in an AnMBR affected the diversity of the microbial community. Further research is required to better understand the effect of changes in the sodium concentration on both anaerobic reactor performance and microbial composition. To the best of our knowledge, all previous studies only investigated a gradual increase in salinity. However, in practice, more drastic salinity fluctuations may occur owing to process operation dynamics, device cleaning, and/or water recycling [16]. Presently, there is very little research on salinity fluctuations in anaerobic reactors, including AnMBRs.

Based on the above considerations, this study aimed to assess the effects of large fluctuations in sodium concentration on the anaerobic conversion capacity and membrane filtration performance in an AnMBR used for treating phenol-containing chemical wastewater. Four operation phases were applied to examine whether salinity variations deteriorate the phenol conversion rate, methanogenic activity, and biomass characteristics, such as particle size, extracellular polymeric substances, and filterability. Moreover, we investigated the effect of salinity fluctuations on microbial community diversity.

2. Material and methods

2.1. Experimental reactor set-up and operation

The experiments were carried out by using laboratory-scale AnMBR reactor with 6.5 L effective volume, equipped with an ultra-filtration side-stream membrane module (Fig. 1.). A tubular polyvinylidene fluoride (PVDF) membrane was used (Pentair, The Netherlands) with dimensions of 5.5 mm inner diameter, 0.64 m length, and 30 nm nominal pore size. The system was equipped with feed, recycle and effluent pumps (120U/DV, 520Du, Watson Marlow, The Netherlands), pH and temperature sensors (Memosens, Endress & Hauser, Germany), biomass recirculation flow meter (Mag-view MVM-030-PN, Bronkhorst, The Netherlands), a permeate scale (EW 2200-2NM, Kern-Sohn, Germany), and a biogas flowmeter (Milligas Counter MGC – 1 PMMA, Ritter, Germany). Transmembrane pressure (TMP) was measured using three pressure sensors (AE Sensors ATM, The Netherlands). Warm water was recirculated by a thermostatic water bath (Tamson Instruments, The Netherlands) through the reactor's water jacket, and the temperature was controlled at 35.0 ± 0.8 °C. The AnMBR was controlled by a computer running LabView software (version 15.0.1f1, National Instruments, USA).

The AnMBR operated as a continuously mixed reactor during 180 days in phases of 40 (phase I-III) and 60 (phase IV) days. The biomass was continuously recirculated at a cross-flow velocity of 0.6 $m.s^{-1}$ with a reactor turnover of about 190 times per day. The sludge of the AnMBR was acclimated to sodium concentrations in the range of 8–22 $gNa^{+}{\cdot}L^{-1}$. The sodium concentration in the AnMBR was varied in each of the four phases of operation as shown in Fig. 2.A. Different modes, simulating

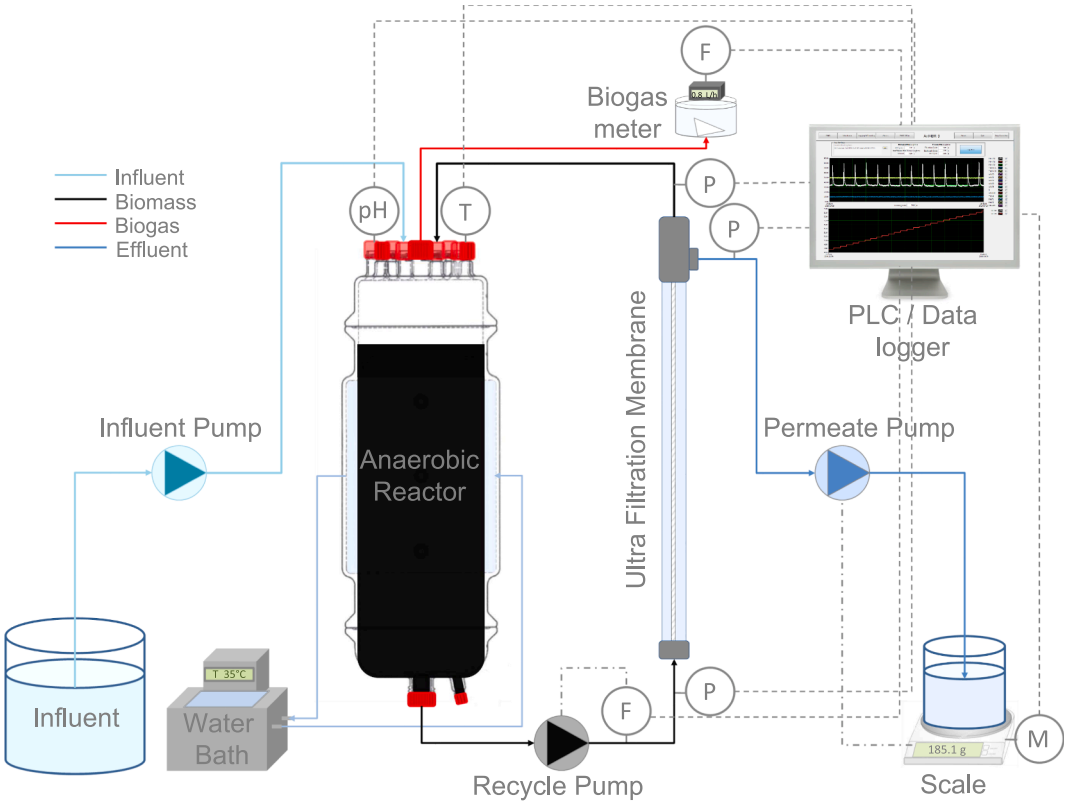

Fig. 1. Schematic representation of the AnMBR.

high salinity variations, were applied, i.e., increasing/decreasing between 18 and 23 $gNa^{+}{\cdot}L^{-1}$, stepwise increase from 20 to 37 $gNa^{+}{\cdot}L^{-1}$, decrease from 37 to 26 $gNa^{+}{\cdot}L^{-1}$, and random fluctuations between 8 and 35 $gNa^{+}{\cdot}L^{-1}$ with different variation frequencies between 2 and 7 days. In phase III, the sodium concentration was kept constant once it reached 26 $gNa^{+}{\cdot}L^{-1}$. In phase IV, the random salinity fluctuations followed a random data set generated with Minitab statistical software (Minitab 17, Minitab LLC). A completely mixed reactor mass balance model was used to determine the sodium feed solution composition in order to reach the desired in-reactor sodium concentrations with a control bulk-liquid volume of 6.5 L.

Sodium mass balance:

$$\frac{dC}{dt} = \frac{Q}{V}Cin - \frac{Q}{V}C \quad (1)$$

With $\frac{Q}{V} = \tau$ and $\frac{dC}{dt} = C^{'}(t)$

Rearranging the equation as a function of time:

$$C^{'}(t) = \tau Cin - \tau C(t) \quad (2)$$

Integrating to solve the Eq. (2) then:

$$C(t) = Cin + ce^{-\tau t} \quad (3)$$

with c as the integration constant:

$$c = C(0) - Cin \quad (4)$$

Therefore, by knowing the actual sodium concentration ($C(0)$) and the final concentration ($C(t)$) that is determined to be reached in the fluctuation within a time (t), the corresponding sodium concentration of the AnMBR feed solution (Cin) and the constant value (c) were calculated.

Table 1 summarizes the operational conditions of the AnMBR continuous flow experiment.

The average SRT of the AnMBR was maintained at about 517 ± 180 days (Table 1).

The reactor was fed with synthetic wastewater containing sodium acetate trihydrated (70.8 $g.L^{-1}$) and phenol (0.5 $gPh.L^{-1}$). The sodium chloride (NaCl), K_2HPO_4 (34.85 $g.L^{-1}$) and KH_2PO_4 (24 $g.L^{-1}$) varied depending on the sodium concentration applied in the reactor maintaining a fixed K^{+}:Na^{+} ratio of 0.05. Macronutrients (9 $mL.L^{-1}$), micronutrients (4.5 $mL.L^{-1}$) and yeast extract (2.0 $g.L^{-1}$) were supplemented. Macronutrients solution included (in $g.L^{-1}$): NH_4Cl 170, $CaCl_2{\cdot}2H_2O$ 8, and $MgSO_4{\cdot}7H_2O$ 9; and micronutrients solution contained (in $g.L^{-1}$): $FeCl_3{\cdot}6H_2O$ 2, $CoCl_2{\cdot}6H_2O$ 2, $MnCl_2{\cdot}4H_2O$ 0.5, $CuCl_2{\cdot}2H_2O$ 0.03, $ZnCl_2$ 0.05, H_3BO_3 0.05, $(NH_4)6Mo_7O_2{\cdot}4H_2O$ 0.09, Na_2SeO_3 0.1, $NiCl_2{\cdot}6H_2O$ 0.05, EDTA 1, Na_2WO_4 0.08.

2.2. Specific methanogenic activity (SMA)

SMA tests were performed in triplicate using an automated methane potential test system (AMPTS, Bioprocess Control, Sweden) and were carried out at 35 °C following the method described by Spanjers and Vanrolleghem [17]. The ratio K^{+}:Na^{+} was kept constant at 0.05 in the media. The initial pH was adjusted to 7.0 (20 ± 0.4 °C).

2.3. Flow cytometry assay

Flow cytometry assay was conducted with biomass samples at different sodium concentrations. BD Accuri C6® flow cytometer (BD Accuri cytometers, Belgium) was used, with a 50 mW laser emitting at a fixed wavelength of 488 nm. BD Accuri CFlow® software was used for data analysis to distinguish between intact cells and cells with compromised membranes. Biomass samples were diluted to obtain bacteria concentrations less than 2×10^5 cells mL^{-1}. Samples were stained and evaluated following the protocol defined by Prest et al. [18].

2.4. Biomass characteristics stress index (BSI)

ATP was measured by QG21Waste™ test kits from biomass samples following the manufacturer's method (Luminultra®). Total ATP (tATP) and dissolved ATP (dATP) were determined to observe the impact of sodium concentration on biomass integrity. The tATP is the sum of intracellular and extracellular ATP and the dATP is the ATP present outside living cells and rejected by dead microorganisms. Analyses were conducted in duplicates. After dilution and extraction steps, samples were read immediately by a luminometer. The biomass stress index (BSI %), which indicates the stress level or mortality of the biomass, was calculated with the equation: BSI [%] = 100 (dATP/tATP) [19].

2.5. Biomass characteristics

2.5.1. Extracellular polymeric substances (EPS) and soluble microbial products (SMP)

EPS and SMP were characterized based on proteins and polysaccharides methods [20,21]. Biomass samples were centrifuged at 4 °C and 12,000 rpm for 15 min. The supernatant was filtered (0.45 μm) and directly used to measure the SMP. EPS extraction was carried out by the cation exchange resin method. DOWEX Marathon C (20–50 μm mesh, sodium form, Fluka 91973) was used as a cation exchange resin. Extraction was carried out at 4 °C, 800 rpm, during 4 h. EPS was normalized against the volatile suspended solids (VSS) concentration of the biomass in the reactor. The VSS and total suspended solids (TSS) concentrations were determined following standard methods using the lowest possible sample volume [22].

2.5.2. Relative hydrophobicity

Biomass relative hydrophobicity (RH) was determined by bacterial adhesion to hydrocarbons method with dodecane as the hydrocarbon phase [23]. Analyses and sampling were conducted in triplicates. 1 g/L TSS of biomass samples was obtained by dilution with permeate. 4 mL dodecane was added to each sample (4 mL) and the resulting suspension was mixed for 1 min. The water phase was taken with a pipette after 10 min gravitational phase separation, and the corresponding absorbance (Abs_f) was determined at 600 nm by a UV spectrophotometer (DR3900, Hach Lange, Germany). The AnMBR permeate was used as the blank and the diluted biomass sample was measured as the initial absorbance (Abs_i). All measurements were carried out in triplicates, and RH was calculated as RH[%] = 100 (1-Abs_f/Abs_i).

2.5.3. Biomass filterability: Capillary suction time (CST)

CST of the biomass was measured by a Capillary Suction Timer device (Model 304 M, Triton Electronics, Essex, England, UK). A CST paper (7 × 9 cm) was used for each sample (6.4 mL). Samples were measured in triplicate. The results were normalized by dividing the CST by total suspended solids concentration [24].

2.5.4. Particle size distribution (PSD)

PSD measurements were carried out employing a DIPA-2000 Eye-Tech™ particle analyzer (Donner Technologies, Or Akiva, Israel) with an A100 and B100 laser lens (0.1–300 μm and 1–2000 μm, respectively) and a liquid flow cell DCM − 104A (10 × 10 mm). The median particle size of the PSD is expressed as D50.

2.6. Permeate characterization

2.6.1. Sodium concentration

Sodium concentrations in the reactor permeate were measured by Ion Chromatography (Metrohm, Switzerland). Dilutions were applied to samples and were prepared in triplicates. Calibration curves were made using standard solutions (Sigma-Aldrich) in the range between 0.1 and 50 $mg{\cdot}L^{-1}$. The final concentrations were calculated by using the MagIC Net 3.2 software.

2.6.2. Phenol and COD analysis

Phenol concentrations were measured by high-performance liquid chromatography HPLC LC-20AT (Shimadzu, Japan) equipped with a 4.6 mm reversed-phase C18 column (Phenomenex, The Netherlands) and a UV detector at a wavelength of 280 nm. The mobile phase was 25% (v/v) acetonitrile solution at a flow rate of 0.95 mL.min^{-1}. The column oven was set at 30 °C. Quick phenol concentration measurements were carried out by Merck – Spectroquant® Phenol cell kits using a spectrophotometer NOVA60 (Merck, Germany). Hach Lange kits were used to measure chemical oxygen demand (COD). Proper dilutions were made to avoid interference by high chloride concentrations, without compromising the accuracy of the measurement. The COD was measured using a VIS - spectrophotometer (DR3900, Hach Lange, Germany).

2.7. Membrane cleaning

At the end of the experiment, the membrane of the AnMBR was cleaned, first physically and then chemically, to determine the different fouling resistances. The physical membrane cleaning was performed by flushing the membrane with water to remove the cake layer. The chemical cleaning was carried out by soaking the membrane in 500 ppm NaClO and 2000 ppm citric acid solution sequentially for 2 h each. After each step, the membrane resistance to water filtration was measured. The total resistance to filtration is formulated as the sum or the intrinsic, removable, irreversible and irrecoverable resistance, $R_{total} = \Delta P_T \cdot \eta \cdot J = R_{intrinsic} + R_{removable} + R_{irreversible} + R_{irrecoverable}$; where R_{total} is the total filtration resistance (m^{-1}), $R_{intrinsic}$ the intrinsic membrane resistance (m^{-1}), $R_{removable}$ the cake layer resistance that is physically removed by flushing with water (m^{-1}), $R_{irreversible}$ the resistance caused by inorganic and organic foulants which is removed by chemical cleaning (m^{-1}), $R_{irrecoverable}$ the resistance caused by foulants that are not removed by physical and chemical cleaning (m^{-1}), and J, ΔP_T and η refer to the flux (m^3·m^{-2}·s^{-1}), transmembrane pressure (TMP) (Pa) and the dynamic viscosity of water (Pa·s), respectively.

2.8. Microbial community analysis

Samples were taken within the four operational phases with intervals ≥ 20 days. The DNA extraction was carried out from AnMBR's biomass samples by using the DNeasy UltraClean Microbial Kit (Qiagen, Hilden, Germany) to evaluate the microbial community dynamics. DNA obtained was checked by agarose gel electrophoresis (quality) and Qubit3.0 DNA detection (Qubit® dsDNA HS Assay Kit, Life Technologies, U.S.) (quantity). 16S rRNA gene amplicon sequencing was carried out by the MiSeq Illumina platform and using the primers 341F (5′-CCTACGGGNGGCWGCAG-3′) 785R (5′-GACTACHVGGGTATCTAATCC-3′) for bacteria/archaea in the V3-V4 region (BaseClear, Leiden, the Netherlands). The QIIME pipeline (version 1.9.0) was used to analyze the sequences [25]. Demultiplexing and quality filtering were performed with parameter values Q = 20, r = 3, and p = 0.75. Chimeric sequences were removed with UCHIME2 (version 9.0) algorithm [26]. Sequences were clustered into operational taxonomic units (OTUs) with a 97% similarity as the cutoff, with UCLUST algorithm [27]. Singletons were removed, and OTUs with an occurrence less than three times in at least one sample were excluded. The taxonomic assignation was performed using the Silva database (SILVA−128) with UCLUST [28]. Alpha diversity was determined after random subsampling using the metrics Chao1, observed OTUs, Shannon, and Simpson indices in QIIME. The sequences reported in this paper have been deposited at ENA under the study accession number PRJEB38420.

3. Results and discussion

3.1. AnMBR process performance

The AnMBR treating phenol-containing wastewater was subjected to sodium concentration fluctuations (Fig. 2A). Phenol removal efficiencies of 99% were achieved at 18–23 gNa$^+$·L^{-1} after 20 days of operation (Phase I, Fig. 2B). The lowest and highest volumetric phenol conversion rates achieved were 78 mgPh·L^{-1}·d^{-1} (7.5 mgPh·gVSS^{-1}·d^{-1}) and 114 mgPh·L^{-1}·d^{-1} (15.0 mgPh·gVSS^{-1}·d^{-1}), respectively (Table 2). Concomitantly, COD removal efficiencies between 96 and 99% were achieved (Phase I, Fig. 2C). The SMA decreased by 21% at the end of phase I from the initial value of 0.39 gCOD-CH4·gVSS^{-1}·d^{-1} (Table 2.).

In phase II, after the sodium concentration reached 37 gNa$^+$·L^{-1} on days 62–79, the phenol removal efficiency decreased from 98% to 86%. The in-situ phenol conversion rate on day 80 was 101 mgPh·L^{-1}·d^{-1} (13

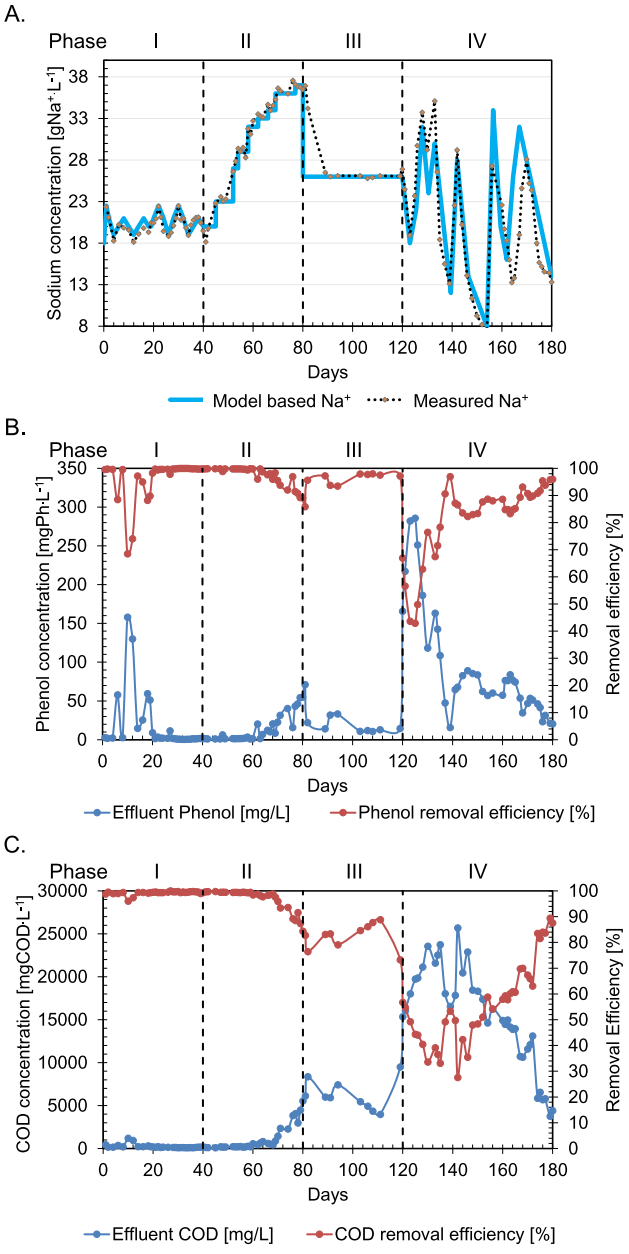

Fig. 2. Anaerobic membrane bioreactor performance. A. Applied sodium concentrations. B. Effluent phenol concentration and removal efficiency. C. Effluent COD concentration and removal efficiency.

Table 1
Operational conditions of the AnMBR.

Parameter	Value	Units
Influent phenol	0.50	$gPh{\cdot}L^{-1}$
OLR	8.07 ± 0.1	$gCOD{\cdot}L^{-1}{\cdot}d^{-1}$
Flow rate	1.48 ± 0.2	$L{\cdot}d^{-1}$
SRT	517 ± 180	d
Flux	5.9 ± 0.8	$L{\cdot}m^{-2}{\cdot}h^{-1}$
Cross flow velocity	0.60	$m{\cdot}s^{-1}$
TMP	80–250 (I-III)	mbar
	>250 (IV)	mbar
Temperature	35.0 ± 0.8	°C
pH	8.1 ± 0.2	pH

$mgPh{\cdot}gVSS^{-1}{\cdot}d^{-1}$). The COD removal efficiency was maintained above 99% at sodium concentrations of up to 26 $gNa^{+}{\cdot}L^{-1}$. However, at the end of phase II, the COD removal efficiency reduced to 84%, corresponding to a COD effluent concentration of 5,445 $mgCOD{\cdot}L^{-1}$ (Phase II, Fig. 2C). The SMA was 0.12 ± 0.05 $gCOD\text{-}CH4{\cdot}gVSS^{-1}{\cdot}d^{-1}$ before COD removal deteriorated at 36.3 $gNa^{+}{\cdot}L^{-1}$. This SMA value was ten-fold higher than that expected based on our previously reported sodium response curve [2], suggesting that the AnMBR biomass was well adapted to high sodium concentrations. Wang et al. [29] also showed a significant decreased in methanogenic activity of 59% by increasing the sodium concentration from 10 to 20 $gNa^{+}{\cdot}L^{-1}$ in a UASB reactor treating phenolic wastewater.

In phase III, sodium concentration was reduced to 26 $gNa^{+}{\cdot}L^{-1}$, and was maintained at a constant level to recover the biomass from reactor perturbation caused by the high salinity built up in phase II. We observed a notably fast recovery in the phenol removal efficiency of 93 – 97% in the remainder of phase III (Phase III, Fig. 2B). In contrast, the COD removal efficiency only slowly recovered with a concomitant increase in SMA to 0.56 ± 0.02 $gCOD\text{-}CH4{\cdot}gVSS^{-1}{\cdot}d^{-1}$. On day 119, a COD removal efficiency of 73% was observed (Phase III, Fig. 2C). The results indicated that compared to phenol conversion, methanogenesis was more severely affected by increasing sodium concentrations. Wu et al. [30] concluded that when increasing the salinity from low (3.3 $mS{\cdot}cm^{-1}$) to high (21.0 $mS{\cdot}cm^{-1}$), the abundance of hydrogenotrophic and acetoclastic methanogens decreased significantly, which resulted in a reduced COD conversion to methane.

In phase IV, when the salinity decreased from 26 to 18.9 $gNa^{+}{\cdot}L^{-1}$ on day 123, the lowest phenol removal efficiency was 43%, and the SMA was 0.05 ± 0.03 $gCOD\text{-}CH4{\cdot}gVSS^{-1}{\cdot}d^{-1}$. On day 140, the sodium concentration decreased to 13 $gNa^{+}{\cdot}L^{-1}$, causing an increase in the phenol removal efficiency to 97%, whereas an increase to 29 $gNa^{+}{\cdot}L^{-1}$ on day 142 decreased the efficiency to 84% (Phase IV, Fig. 2B). A subsequent decrease to 8 $gNa^{+}{\cdot}L^{-1}$ resulted in an increase in the phenol removal efficiency increase to 87%. Vyrides et al. [31] also suggested an improved process performance after a step-wise decrease from 13.8 $gNa^{+}{\cdot}L^{-1}$ to 0.08 $gNa^{+}{\cdot}L^{-1}$ in a submerged AnMBR. We noted that the consecutive large fluctuations to 27, 13, 28 and 13 $gNa^{+}{\cdot}L^{-1}$ (Phase IV, Fig. 2A) did not have a negative effect on the phenol removal efficiency that increased from 83% to 95% at the end of phase IV. The phenol conversion rate increased from 50 (6.9 $mgPh{\cdot}gVSS^{-1}{\cdot}d^{-1}$) to 109 $mgPh{\cdot}L^{-1}{\cdot}d^{-1}$ (25.5 $mgPh{\cdot}gVSS^{-1}{\cdot}d^{-1}$) during phase IV. Fluctuating the sodium concentrations between 13 and 35 $gNa^{+}{\cdot}L^{-1}$, revealed a decreasing trend in the COD removal efficiency with the minimum value reaching 28% on day 142. However, further fluctuations up to day 180 did not negatively affect the COD removal efficiency. In contrast, a gradual recovery of up to 88% was observed (Phase IV, Fig. 2C). Concurrently, the SMA increased to 0.39 ± 0.05 at a sodium concentration of 16.0 $gNa^{+}{\cdot}L^{-1}$ (Table 2). Previous studies on AnMBRs at high salinity suggested that step-wise increases in sodium concentration of up to 16 $gNa^{+}{\cdot}L^{-1}$ reduced the COD removal efficiency to values lower than 80% [9,10]. Moreover, small salinity fluctuations of 2 $gNa^{+}{\cdot}L^{-1}$ between 18 and 20 $gNa^{+}{\cdot}L^{-1}$ were previously assessed, which did not affect the overall AnMBR conversion performance [11]. In contrast, despite the application of high salinities (8–37 $gNa^{+}{\cdot}L^{-1}$), the results suggested that the microbial community became more resilient to disturbances caused by large fluctuations in salinity. As a result, the AnMBR phenol and COD conversion capacities were sustained and recovered, respectively, to values higher than 88%.

The flow cytometry results showed that most cells (84%) with compromised membranes were observed after the salinity increased from 20 to 37 $gNa^{+}{\cdot}L^{-1}$ at the beginning of phase III (Fig. 3A). Moreover, during the large fluctuations in the range of 8–37 $gNa^{+}{\cdot}L^{-1}$ (phase IV), 67% of cells had compromised membranes on day 146. On the contrary, the number of cells with compromised membranes was only 15% in phase I and approximately 20% at the end of phase IV, corresponding to the highest phenol and COD removal efficiencies in the AnMBR. By measuring the dissolved ATP over total ATP, the biomass stress index (BSI) was determined, which reflects the microbial stress level of the biomass and indicates the deterioration of the biological process [19] (Fig. 3B). Biomass samples from phase I showed a relatively low BSI with an average of 38%. During phase II, and increasing trend from 39% to 99% was observed with a step-wise increased in salinity to 37 $gNa^{+}{\cdot}L^{-1}$. A decrease to a BSI of 50% was attained when no salinity fluctuations were imposed on the reactor in phase III, which can be considered indicative of microbial adaptation and cell recovery [32]. In addition, osmoprotectants present in the yeast extract and protein (PN)-like substances may have played a role in alleviating the osmotic stress of the anaerobic biomass [33]. In phase IV, the BSI index was unstable and increased up to 99%, following biomass exposure to fluctuations in sodium concentrations exceeding 14 $gNa^{+}{\cdot}L^{-1}$. Hereafter, the BSI decreased to 49% at sodium concentrations in the range of 8–28 $gNa^{+}{\cdot}L^{-1}$.

3.2. Effect of salinity fluctuations on biomass characteristics

3.2.1. Extracellular polymeric substances (EPS) and soluble microbial products (SMP)

Proteins (PN) and polysaccharides (PS) were determined as the main compounds in EPS and SMP in the AnMBR. EPS-PN accounted for 82% of the total EPS, with their content being 5 $mg{\cdot}gVSS^{-1}$ at the initial sodium concentration of 22.4 $gNa^{+}{\cdot}L^{-1}$ (Table 3.). Salinity fluctuations in phase

Table 2
Specific methanogenic activity, as well as volumetric and specific phenol conversion rate at different sodium concentrations in the four operational phases of the AnMBR.

Phase	Day	Sodium concentration [$gNa^{+}{\cdot}L^{-1}$]	SMA [$gCOD\text{-}CH_4gVSS^{-1}{\cdot}d^{-1}$]	Phenol conversion rate [$mgPh{\cdot}L^{-1}{\cdot}d^{-1}$]	Min. and Max. phenol conversion rates [$mgPh{\cdot}L^{-1}{\cdot}d^{-1}$]	Specific phenol conversion rate [$mgPh{\cdot}gVSS^{-1}{\cdot}d^{-1}$]
I	1	22.3	0.39 ± 0.00	113	$78^{Min}114^{Max}$	10.7
	30	22.5	0.31 ± 0.03	114		15.0
II	70	36.3	0.12 ± 0.05	109	$101^{Min}114^{Max}$	14.3
III	101	26.1	0.56 ± 0.02	111	$98^{Min}111^{Max}$	15.1
IV	123	18.9	0.50 ± 0.10	50	$49^{Min}110^{Max}$	6.9
	137	15.5	0.05 ± 0.03	103		18.6
	163	16.0	0.39 ± 0.05	95		12.6
	180	13.3	0.28 ± 0.04	109		25.5

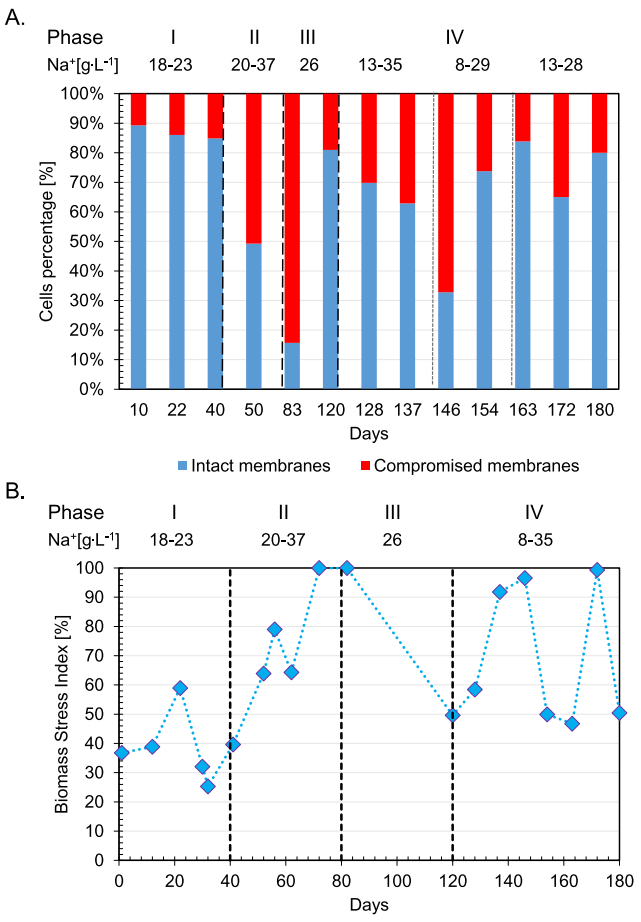

Fig. 3. A. Cells percentage with intact and compromised membranes. B. Biomass stress index (BSI).

Table 3
EPS and SMP concentrations resulting from salinity fluctuations. PN: Proteins, PS: Polysaccharides.

Phase	Day	Sodium concentration [$gNa^{+}{\cdot}L^{-1}$]	EPS [$mg{\cdot}gVSS^{-1}$]		SMP [$mg{\cdot}gVSS^{-1}$]	
			PS	PN	PS	PN
I	0	22.4	1.1	5.0	0.7	24.2
	14	19.1	0.4	32.3	0.1	127.8
	28	20.1	0.2	26.1	0.3	51.0
	40	19.5	2.1	35.2	0.0	14.0
II	54	29.4	1.9	30.3	1.7	62.9
	68	34.6	2.4	42.5	1.6	72.5
III	80	36.9	0.9	22.8	2.3	136.6
IV	120	26.9	2.6	65.6	5.1	154.3
	137	15.5	5.6	62.6	2.5	112.3
	146	14.1	6.3	75.6	2.3	128.9
	154	8.0	8.0	118.6	3.1	128.7
	163	16.0	10.0	113.2	2.9	163.7
	172	24.4	5.2	68.9	2.8	87.8
	180	13.3	7.0	91.2	1.2	64.5

I (18–23 $gNa^{+}.L^{-1}$) increased the EPS-PN content from 5.0 to 35.2 $mg{\cdot}gVSS^{-1}$. However, the EPS-PS content did not significantly increase in both phase II and III. Similarly, Ismail et al. [7] reported that the PN fraction of EPS in a UASB operated at 20 $gNa^{+}{\cdot}L^{-1}$ was much higher, i.e., 87–94%, than the PS fraction. The exposure to increased salinity in the AnMBR biomass in phase II increased the PN content of EPS to 42.5 $mg{\cdot}gVSS^{-1}$; however, it decreased to 22.8 $mg{\cdot}gVSS^{-1}$ when the sodium concentration in the reactor reached 36.9 $gNa^{+}{\cdot}L^{-1}$ on day 80. Concomitantly, the SMP-PN content increased from 14 $mg{\cdot}gVSS^{-1}$ at 19.5 $gNa^{+}{\cdot}L^{-1}$ to 136.6 $mg{\cdot}gVSS^{-1}$ at the end of phase II, suggesting protein solubilization due to high salinity exposure [34]. During random fluctuations in phase IV, the highest amount of EPS-PN of 118.6 $mg{\cdot}gVSS^{-1}$ was observed under the fluctuation from 14 to 8 $gNa^{+}{\cdot}L^{-1}$. For SMP-PN, the highest PN concentration was 163.7 $mg{\cdot}gVSS^{-1}$ on day 163, after the variation from 27 to 16 $gNa^{+}{\cdot}L^{-1}$. We noted foaming in the AnMBR within this phase. Foaming might be attributed to the increase in proteins at the gas/liquid interface owing to their surface-active properties [35].

3.2.2. *Relative hydrophobicity (RH)*

The RH of the AnMBR biomass during phases I, II, III, and IV was, on average, 37 ± 15%, 44 ± 5%, 35 ± 19%, and 11 ± 5%, respectively (Fig. 4.). The biomass was highly hydrophobic at the start of phase I as well as after being exposed to a high sodium concentration (36.9 $gNa^{+}{\cdot}L^{-1}$) at the end of phase II. High content of EPS-PN is generally responsible for high biomass hydrophobicity. In contrast, large salinity fluctuations in phase IV decreased AnMBR biomass hydrophobicity to 8%, even though extracellular PN-like substances were higher than PS. The low hydrophobicity of the AnMBR biomass in phase IV, likely resulted in increased cake/gel layer accumulation on the hydrophilic membranes and therefore to a higher transmembrane pressure. Reversely, Van den Broeck et al. [36] reported that an increase in biomass hydrophobicity resulted in decreased membrane fouling, which can be attributed to a reduced interaction between hydrophobic biomass and usually hydrophilic membranes.

3.2.3. *Biomass particle size and capillary suction time (CST)*

The median biomass particle size (D50) decreased by approximately 45% from 21.0 μm at the start of phase I (22.4 $gNa^{+}{\cdot}L^{-1}$) to 11.5 μm at the end of phase I (Fig. 4). In phase II, along with the step-wise increase in salinity to 37 $gNa^{+}{\cdot}L^{-1}$, D50 increased to 19.4 μm on day 80. Ismail et al. [7] and Gagliano et al. [37], assessed granular sludge in UASB reactors, and observed that granules formed at 20 $gNa^{+}{\cdot}L^{-1}$ were bigger than those formed at 10 $gNa^{+}{\cdot}L^{-1}$. The high concentration of sodium might weaken the binding of EPS and induce enlarged flocs, resulting in a likely weaker structure.

In phase III, the median particle size increased to 65.6 μm , under a constant sodium concentration of 26 $gNa^{+}{\cdot}L^{-1}$. However, a total reduction of 93.4% in the D50 to 4.3 μm from the beginning to the end of phase IV notably indicated a substantial negative effect on the biomass particle size due to the large salinity fluctuations. Moreover, Liu and

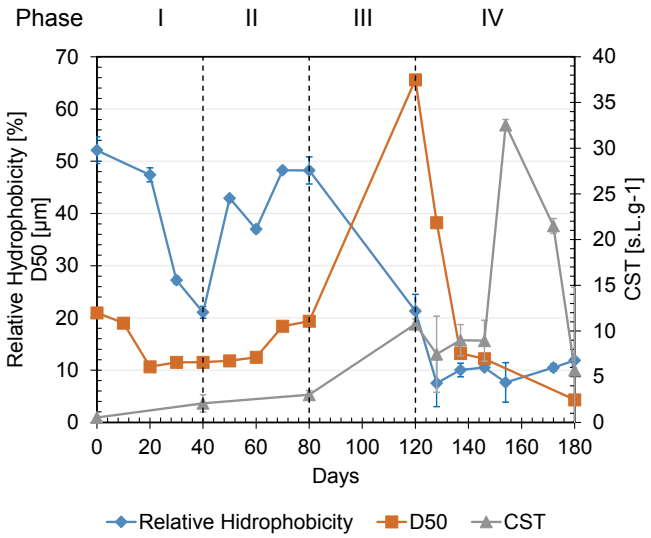

Fig. 4. Left y-axis: Relative hydrophobicity [%] and median biomass particle size D50 [μm]. Right y-axis: Normalized capillary suction time [$s.L.g^{-1}$].

Fang [38] concluded that a reduction in the biomass particle size could also result from a decreasing sludge hydrophobicity, as was observed in phase IV. Although a decrease in biomass particle size under increasing salinity conditions is observed by other studies [12,39], our present results clearly show the detrimental effects of large salinity fluctuations on biomass morphology.

CST ranged from 0.5 $s{\cdot}L{\cdot}gTSS^{-1}$ in phase I to 32.5 $s{\cdot}L{\cdot}gTSS^{-1}$ in phase IV. These results corroborated with those described above of D50. When the biomass was exposed to 8 $gNa^{+}{\cdot}L^{-1}$ on day 154, the measured CST (32.5 $s{\cdot}L{\cdot}gTSS^{-1}$) was three times higher than the initially observed 10.8 $s{\cdot}L{\cdot}gTSS^{-1}$ on day 120, which corresponded the major decrease in particle size in phase IV. This increased in CST indicated that the biomass had the worst filterability characteristics after being exposed to large salinity fluctuations in phase IV, which contributed to an increasing resistance to filtration.

3.3. Membrane filtration performance

The AnMBR exhibited a non-disturbed filtration performance in phases I, II, and III, when the reactor was operated under a transmembrane pressure (TMP) of 80 to 250 mbar and an average flux of 5.9 $L.m^{-2}.h^{-1}$. A TMP of 250 mbar was reached in phase II, while operating the AnMBR at 37 $gNa^{+}{\cdot}L^{-1}$. However, in phase IV, when sodium concentrations between 29 and 35 $gNa^{+}{\cdot}L^{-1}$ were applied (days 120–137), the TMP rapidly increased to 452 mbar (day 133), concomitantly with a membrane filtration resistance increase to 26.1 $\times$ 10^{12} m^{-1} (Fig. 5A). The deterioration of the membrane filtration performance was attributed to the decrease in biomass particle size from 65.6 to 13.2 μm (Fig. 4). The TMP and membrane filtration resistance increased gradually, reaching peaks on days 138, 148, and 156. The change from 8 to 27.3 $gNa^{+}{\cdot}L^{-1}$ apparently led to an increase in the TMP and membrane resistance to filtration reaching 667 mbar and 38 $\times$ 10^{12} m^{-1}, respectively on day 156. After day 163, TMP gradually increased further up to 774 mbar at the end of AnMBR operation, with a particle size reduction from 12.2 to 4.3 μm. Zhou et al. [40] indicated that particles in the range 0.45–10 μm are the main foulants in AnMBRs, and especially particles in the size-fraction from 5 to 10 μm led to higher cake resistances. Hence, the low biomass particle size at the end of our experiment most likely contributed to cake layer compaction and, thereby, to a higher resistance to filtration.

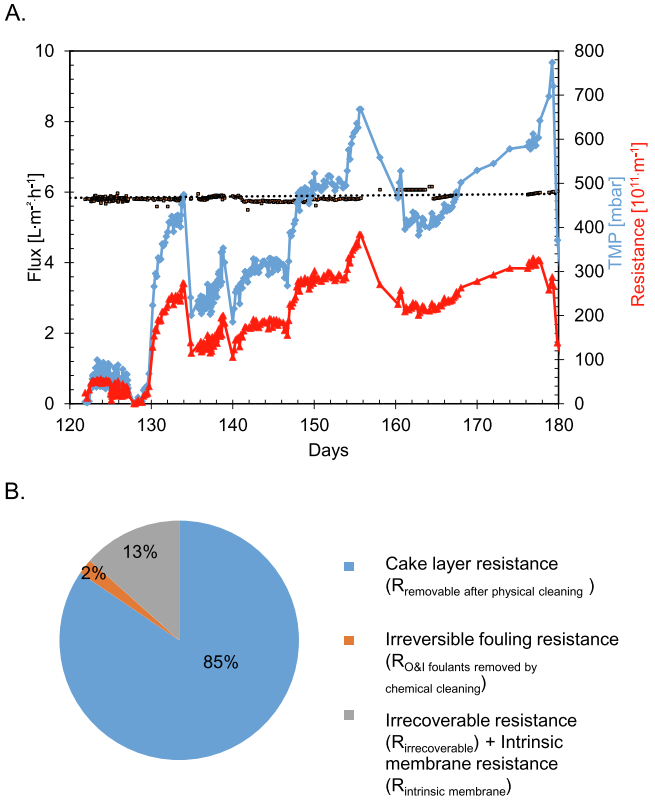

Fig. 5. A. Membrane filtration performance during large salinity fluctuations in phase IV. B. Relative contribution of the different types of fouling to the total filtration resistance at the end of the experiment.

Fig. 5B shows the relative contributions of the different types of fouling to the total resistance to filtration in AnMBR at the end of the experiment. Cake layer resistance compromised the largest portion of total filtration resistance, i.e., 85%, which confirmed that the primary fouling mechanism in the AnMBR was cake layer formation. Sequential chemical cleaning conducted using NaClO and citric acid resulted in an increase in the membrane permeability of only 2%. Complete restoration of the membrane permeability was not possible, and 13% of the permeability loss was attributed to both intrinsic and irrecoverable fouling. Both the role of osmotic pressure changes on filtration resistance [41] and gel layer formation mechanisms due to high SMP accumulation [42], resulting from salinity fluctuations, should be investigated further.

3.4. Microbial community diversity and dynamics

The microbial community dynamics of the reactor biomass was determined in the four phases of the AnMBR operation. Alpha diversity indices [43] were used to compare the evenness and richness of the microbial population in the reactor (Fig. 6). The alpha diversity metrics from the Chao1 index slightly decreased at the end of phase I on day 40 from 611 to 586. An increasing trend to 649 and 666 in phases II and III, respectively, and up to 707 in phase IV on day 142 was observed. The observed OTUs showed a similar trend (Fig. 6A). The Chao1 (498) and observed OTUs (383) scores showed that at the end of AnMBR operation, the number of OTUs was lower than the initial and maximum values observed on days 0 and 142, respectively. This, indicated that larger salinity fluctuations had a considerable effect on the microbial population diversity. However, both scores were high compared with those noted in our previous study [11], where a maximum sodium concentration of 20 $gNa^{+}{\cdot}L^{-1}$ was applied. Both the Shannon's and Simpson's index scores, consider the richness and evenness of the microbial population. The highest values were observed in phase IV on day 163 when a sodium concentration of 16 $gNa^{+}{\cdot}L^{-1}$ was applied (Fig. 6B, C). The decrease in the bacterial diversity (Simpson's = 0.85; Shannon's = 4.33) at the end of the operation indicated a high stress level, which was attributed to the sodium concentration fluctuations exceeding 14 $gNa^{+}{\cdot}L^{-1}$ within four days.

A lower evenness of the microbial community at high stress levels could be caused by the dominance of a few halophilic/salt-tolerant microorganisms. Disturbances, e.g., large salinity fluctuations, could promote higher diversity but could also lead to variable microbial community function. However, we cannot assume that a more diverse community yields a community with better functionality [44]. Under the disturbances caused by different frequencies and concentrations of sodium in the AnMBR in phase IV, a higher alpha diversity did not suggest a healthier system, but on the contrary, the COD conversion gradually increased, whereas there was a decrease in the microbial community diversity in the reactor.

The most dominant bacteria in the AnMBR during the entire operation belonged to class Clostridia (25.2%), Synergistia (16.9%), and Bacteroidia (7.9%), while the dominant archaea were Methanomicrobia (27.9%) and Methanobacteria (11.8%) (Fig. 7A). Na et al. [45] also reported that most detected bacteria in a UASB reactor treating phenols belonged to class Clostridia. Two major population changes were observed following salinity fluctuations in AnMBR. Bacteria belonging to Bacteroidia remarkably increased from 1.8% to 25.1% relative abundance during phase II to III, respectively, and thereafter decreased

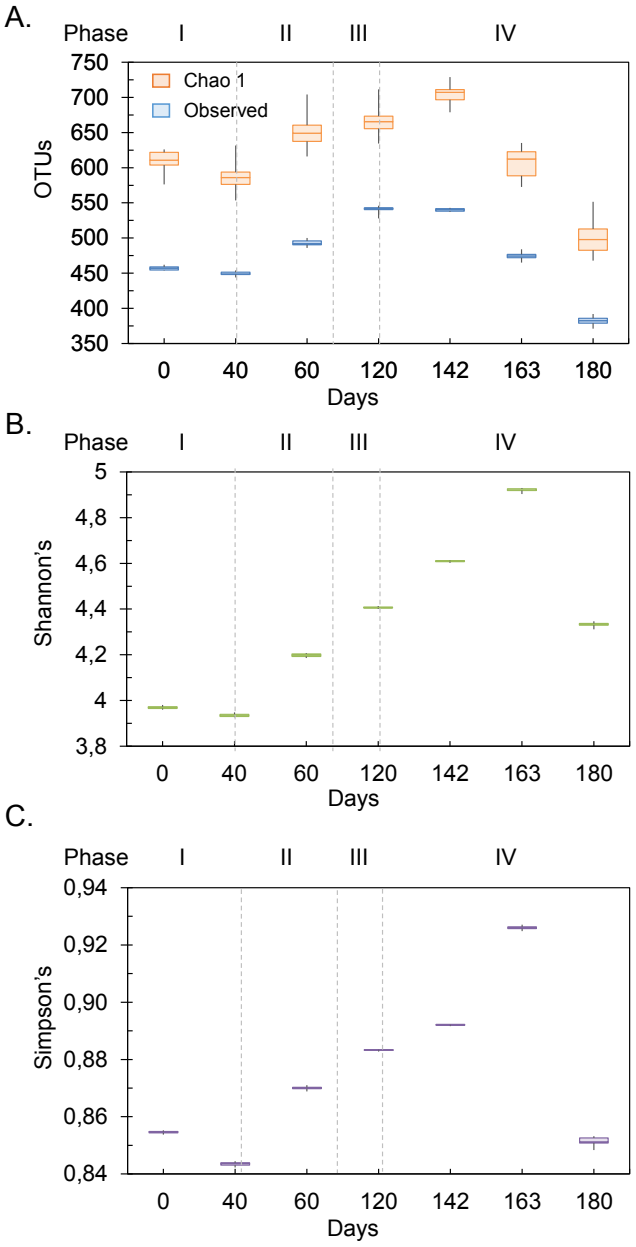

Fig. 6. Alpha diversity plots for the microbial community in AnMBR at different phases of operation. A. Chao1 index and Observed OTU numbers B. Simpson's index C. Shannon's index.

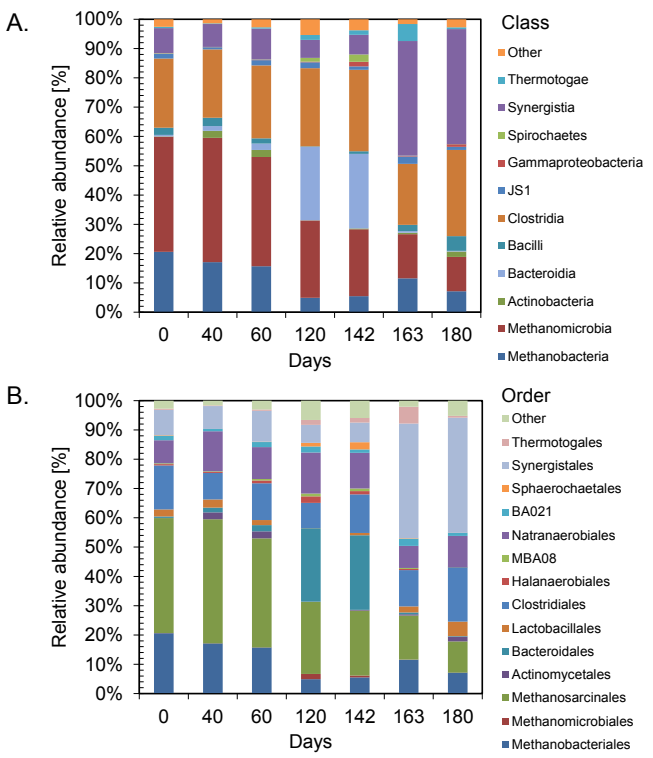

Fig. 7. Microbial community dynamics in AnMBR at the A. Class, B. Order level.

to 2.1% in phase IV, whereas Synergistia increased from 6.7% to 39.3% during phase IV. At the order level, Methanobacteriales and Methanosarcinales decreased from 20.6% and 39.3%, respectively, on day 0 to 15.7% and 37.2%, respectively, under 33 $gNa^{+}{\cdot}L^{-1}$ in phase II (Fig. 7B). In phases III and IV, Methanobacteriales further decreased to 12.6% and 10.6%, and Methanosarcinales decreased to 10.8% and 7.1, respectively. The highest relative abundance of Methanomicrobiales on day 120 was 1.8%. Along with the large salinity fluctuations in phase IV, Clostridiales increased from 8.6% to 18.6%, while Natranaerobiales decreased from 14.0% to 10.6%. All Synergistales were from the genus *Thermovirgaceae*, whose abundance notably increased from 6.1% to 38.7% in phase IV (see Supplementary material Fig. S1). *Thermovirgaceae* members have a high tolerance to high salinity [46] and a preference for PN/amino acid degradation corresponding to the highest soluble PN (SMP-PN) content observed in phase IV. Similarly, all Bacteroidales were from genus *ML635J-40,* which decreased from 25.0% at the beginning of phase IV to 0.2% at the end. The abundance of *Clostridium*, belonging to Clostridiales, varied between 2.3% and 8.9% during phase IV. The maximum relative abundance of *Pelotomaculum* at 0.9% was observed on day 142 under 29 $gNa^{+}{\cdot}L^{-1}$ in phase IV. In our previous study [11], we related the improvement in the phenol conversion rate to *Pelotomaculum* relative abundance, which, in this study, corresponded with the highest phenol removal observed in phase IV.

3.5. Implications and future research

The large salinity fluctuations affected the conversion capacity of the AnMBR but resulted in increasing resilience to more frequent and larger concentration fluctuations. Although sodium concentrations higher than 26 $gNa^{+}{\cdot}L^{-1}$ and large fluctuations between 8 and 35 $gNa^{+}{\cdot}L^{-1}$ transiently reduced the biomass activity, the reactor preserved a high conversion and recovery capacity. Notably, and to the best of our knowledge, no other anaerobic reactor system, including AnMBRs, have been subjected to sodium concentrations higher than three times the typical seawater sodium concentration (10.5 $gNa^{+}{\cdot}L^{-1}$), with continuous concentration fluctuations exceeding 14 $gNa^{+}{\cdot}L^{-1}$.

Overall, the exhibited robustness of the AnMBR to the large sodium concentration fluctuations would imply a forward step in pushing the limits of high-rate anaerobic bioconversion of industrial chemical wastewaters under highly variable saline conditions, as well as supporting research developments on anaerobic treatment, e.g., of concentrated streams resulting from applying forward osmosis or brines with high organic content. Further research should examine the impact of more frequent salinity fluctuations at a lower hydraulic retention time. Similarly, online control strategies to optimize membrane filtration performance and mitigate the reduction of the biomass particle size due to salinity fluctuations; e.g., applying flux enhancers, should be investigated to guarantee sustainable fluxes at full-scale applications.

4. Conclusions

The AnMBR revealed high robustness against large salinity fluctuations, maintaining phenol conversion rates between 6.9 and 25.5 $mgPh \cdot gVSS^{-1} \cdot d^{-1}$. Sodium concentrations exceeding 26 $gNa^{+} \cdot L^{-1}$ and large sodium fluctuations between 8 and 35 $gNa^{+} \cdot L^{-1}$ resulted in biomass stress and reduced the biomass methanogenic activity and cell membrane integrity. A reduction in median biomass particle size from 21 to 4.3 μm compromised membrane filtration performance and induced transmembrane pressures above 400 mbar. Cake layer resistance contributed to 85% of the total filtration resistance while only 2% irreversible fouling was determined. Microbial population richness and diversity were substantially reduced by salinity fluctuations larger than 14 $gNa^{+} \cdot L^{-1}$. Furthermore, the dominant Bacteria belonging to the orders Clostridiales and Synergistales were enriched, whereas Archaea classified under the orders Methanosarcinales and Methanobacteriales decreased in relative abundance. Nonetheless, there was a gradual increase in COD conversion to 88%. This study revealed the potential of AnMBRs to endure extreme salinity fluctuations, advancing high-rate anaerobic treatment of industrial chemical wastewaters under these conditions.

Declaration of Competing Interest

The authors declare that they have no known competing financial interests or personal relationships that could have appeared to influence the work reported in this paper.

Acknowledgments

This research is supported by the Dutch Technology Foundation (STW, Project No.13348), which is part of the Netherlands Organization for Scientific Research (NWO), partly funded by the Dutch Ministry of Economic Affairs. This research is co-sponsored by Evides Industriewater B.V and Paques B.V. The authors thank the intern students Emilien Herve and Basak Donmez for their laboratory analysis support during different phases of this study. Julian also thanks Frans Willem Hamer for helping with the Python script for membrane filtration data processing, and KWR Water Research Institute for the time provided to complete this manuscript.

Appendix A. Supplementary data

Supplementary data to this article can be found online at https://doi.org/10.1016/j.cej.2021.129263.

References

[1] Z. Kong, L. Li, Y. Xue, M. Yang, Y.-Y. Li, Challenges and prospects for the anaerobic treatment of chemical-industrial organic wastewater: A review, J. Clean. Prod. 231 (2019) 913–927.
[2] J.D. Muñoz Sierra, C. Lafita, C. Gabaldón, H. Spanjers, J.B. van Lier, Trace metals supplementation in anaerobic membrane bioreactors treating highly saline phenolic wastewater, Bioresour. Technol. 234 (2017) 106–114.
[3] O. Lefebvre, F. Habouzit, V. Bru, J.P. Delgenes, J.J. Godon, R. Moletta, Treatment of hypersaline industrial wastewater by a microbial consortium in a sequencing batch reactor, Environ. Technol. 25 (2004) 543–553.
[4] R.K. Dereli, M.E. Ersahin, H. Ozgun, I. Ozturk, D. Jeison, F. van der Zee, J.B. van Lier, Potentials of anaerobic membrane bioreactors to overcome treatment limitations induced by industrial wastewaters, Bioresour. Technol. 122 (2012) 160–170.
[5] M.C. Gagliano, T.R. Neu, U. Kuhlicke, D. Sudmalis, H. Temmink, C.M. Plugge, EPS glycoconjugate profiles shift as adaptive response in anaerobic microbial granulation at high salinity, Front. Microbiol. 9 (2018).
[6] I. Vyrides, D.C. Stuckey, Effect of fluctuations in salinity on anaerobic biomass and production of soluble microbial products (SMPs), Biodegradation 20 (2009) 165–175.
[7] S.B. Ismail, C.J. de La Parra, H. Temmink, J.B. van Lier, Extracellular polymeric substances (EPS) in upflow anaerobic sludge blanket (UASB) reactors operated under high salinity conditions, Water Res. 44 (2010) 1909–1917.
[8] D. Sudmalis, M.C. Gagliano, R. Pei, K. Grolle, C.M. Plugge, H.H.M. Rijnaarts, G. Zeeman, H. Temmink, Fast anaerobic sludge granulation at elevated salinity, Water Res. 128 (2018) 293–303.
[9] X. Song, J. McDonald, W.E. Price, S.J. Khan, F.I. Hai, H.H. Ngo, W. Guo, L. D. Nghiem, Effects of salinity build-up on the performance of an anaerobic membrane bioreactor regarding basic water quality parameters and removal of trace organic contaminants, Bioresour. Technol. 216 (2016) 399–405.
[10] L. Chen, Q. Hu, X. Zhang, Z. Chen, Y. Wang, S. Liu, Effects of salinity on the biological performance of anaerobic membrane bioreactor, J. Environ. Manage. 238 (2019) 263–273.
[11] J.D. Muñoz Sierra, M.J. Oosterkamp, W. Wang, H. Spanjers, J.B. van Lier, Impact of long-term salinity exposure in anaerobic membrane bioreactors treating phenolic wastewater: Performance robustness and endured microbial community, Water Res. 141 (2018) 172–184.
[12] J.D. Muñoz Sierra, M.J. Oosterkamp, W. Wang, H. Spanjers, J.B. van Lier, Comparative performance of upflow anaerobic sludge blanket reactor and anaerobic membrane bioreactor treating phenolic wastewater: Overcoming high salinity, Chem. Eng. J. 366 (2019) 480–490.
[13] B. Rincón-Llorente, D. De la Lama-Calvente, M.J. Fernández-Rodríguez, R. Borja-Padilla, Table olive wastewater: Problem, treatments and future strategy. A review, Front. Microbiol. 9 (2018).
[14] X. Tan, I. Acquah, H. Liu, W. Li, S. Tan, A critical review on saline wastewater treatment by membrane bioreactor (MBR) from a microbial perspective, Chemosphere 220 (2019) 1150–1162.
[15] Q. Lu, Z. Yu, S. Yu, Z. Liang, H. Li, L. Sun, S. Wang, Organic matter rather than salinity as a predominant feature changes performance and microbiome in methanogenic sludge digesters, J. Hazard. Mater. 377 (2019) 349–356.
[16] I. Vyrides, Anaerobic Treatment of Organic Saline Waste/Wastewater: Overcome Salinity Inhibition by Addition of Compatible Solutes, in: L. Sukla, N. Pradhan, S. Panda, B. Mishra (Eds.), Environmental Microbial Biotechnology, Soil Biology, Springer, Cham, 2015.
[17] H. Spanjers, P. Vanrolleghem, Respirometry, in: W.I. Online (Ed.) In: van Loosdrecht et al. Experimental methods in wastewater treatment Water Intell. Online 2016, pp. 360.
[18] E.I. Prest, F. Hammes, S. Kötzsch, M.C.M. van Loosdrecht, J.S. Vrouwenvelder, Monitoring microbiological changes in drinking water systems using a fast and reproducible flow cytometric method, Water Res. 47 (2013) 7131–7142.
[19] M.J. Luján-Facundo, J. Fernández-Navarro, J.L. Alonso-Molina, I. Amorós-Muñoz, Y. Moreno, J.A. Mendoza-Roca, L. Pastor-Alcañiz, The role of salinity on the changes of the biomass characteristics and on the performance of an OMBR treating tannery wastewater, Water Res. 142 (2018) 129–137.
[20] M. Dubois, K.A. Gilles, J.K. Hamilton, P.A. Rebers, F. Smith, Colorimetric method for determination of sugars and related substances, Anal. Chem. 28 (1956) 350–356.
[21] B. Frølund, R. Palmgren, K. Keiding, P.H. Nielsen, Extraction of extracellular polymers from activated sludge using a cation exchange resin, Water Res. 30 (1996) 1749–1758.
[22] A. American Public Health, A.D. Eaton, A. American Water Works, F. Water Environment, Standard methods for the examination of water and wastewater, APHA-AWWA-WEF, Washington, D.C., 2005.
[23] M. Rosenberg, D. Gutnick, E. Rosenberg, Adherence of bacteria to hydrocarbons: A simple method for measuring cell-surface hydrophobicity, FEMS Microbiol. Lett. 9 (1980) 29–33.
[24] S. Jamal Khan, C. Visvanathan, V. Jegatheesan, R. BenAim, Influence of mechanical mixing rates on sludge characteristics and membrane fouling in MBRs, Sep. Sci. Technol. 43 (2008) 1826–1838.
[25] J.G. Caporaso, J. Kuczynski, J. Stombaugh, K. Bittinger, F.D. Bushman, E. K. Costello, N. Fierer, A.G. Pena, J.K. Goodrich, J.I. Gordon, G.A. Huttley, S. T. Kelley, D. Knights, J.E. Koenig, R.E. Ley, C.A. Lozupone, D. McDonald, B. D. Muegge, M. Pirrung, J. Reeder, J.R. Sevinsky, P.J. Turnbaugh, W.A. Walters, J. Widmann, T. Yatsunenko, J. Zaneveld, R. Knight, QIIME allows analysis of high-throughput community sequencing data, Nat. Meth. 7 (2010) 335–336.
[26] R. Edgar, UCHIME2: Improved chimera prediction for amplicon sequencing, bioRxiv (2016).
[27] R.C. Edgar, Search and clustering orders of magnitude faster than BLAST, Bioinformatics 26 (2010) 2460–2461.
[28] D. McDonald, M.N. Price, J. Goodrich, E.P. Nawrocki, T.Z. Desantis, A. Probst, G. L. Andersen, R. Knight, P. Hugenholtz, An improved Greengenes taxonomy with explicit ranks for ecological and evolutionary analyses of bacteria and archaea, ISME J. 6 (2012) 610–618.
[29] W. Wang, B. Wu, S. Pan, K. Yang, Z. Hu, S. Yuan, Performance robustness of the UASB reactors treating saline phenolic wastewater and analysis of microbial community structure, J. Hazard. Mater. 331 (2017) 21–27.
[30] Y. Wu, X. Wang, M.Q.X. Tay, S. Oh, L. Yang, C. Tang, B. Cao, Metagenomic insights into the influence of salinity and cytostatic drugs on the composition and functional genes of microbial community in forward osmosis anaerobic membrane bioreactors, Chem. Eng. J. 326 (2017) 462–469.
[31] I. Vyrides, H. Santos, A. Mingote, M.J. Ray, D.C. Stuckey, Are compatible solutes compatible with biological treatment of saline wastewater? Batch and continuous studies using submerged anaerobic membrane bioreactors (SAMBRs), Environ. Sci. Technol. 44 (2010) 7437–7442.
[32] M. John, A.P. Trzcinski, Y. Zhou, W.J. Ng, Microbial stress mediated intercellular nanotubes in an anaerobic microbial consortium digesting cellulose, Sci. Rep. 7 (2017) 18006.
[33] D. Sudmalis, S.K. Millah, M.C. Gagliano, C.I. Butré, C.M. Plugge, H.H.M. Rijnaarts, G. Zeeman, H. Temmink, The potential of osmolytes and their precursors to

alleviate osmotic stress of anaerobic granular sludge, Water Res. 147 (2018) 142–151.
[34] K.N. Yogalakshmi, K. Joseph, Effect of transient sodium chloride shock loads on the performance of submerged membrane bioreactor, Bioresour. Technol. 101 (2010) 7054–7061.
[35] N. Ganidi, S. Tyrrel, E. Cartmell, Anaerobic digestion foaming causes – A review, Bioresour. Technol. 100 (2009) 5546–5554.
[36] R. Van den Broeck, P. Krzeminski, J. Van Dierdonck, G. Gins, M. Lousada-Ferreira, J.F.M. Van Impe, J.H.J.M. van der Graaf, I.Y. Smets, J.B. van Lier, Activated sludge characteristics affecting sludge filterability in municipal and industrial MBRs: Unraveling correlations using multi-component regression analysis, J. Membr. Sci. 378 (2011) 330–338.
[37] M.C. Gagliano, S.B. Ismail, A.J.M. Stams, C.M. Plugge, H. Temmink, J.B. Van Lier, Biofilm formation and granule properties in anaerobic digestion at high salinity, Water Res. 121 (2017) 61–71.
[38] Y. Liu, H.H.P. Fang, Influences of extracellular polymeric substances (EPS) on flocculation, settling, and dewatering of activated sludge, Crit. Rev. Environ. Sci. Technol. 33 (2003) 237–273.
[39] J. De Vrieze, M. Coma, M. Debeuckelaere, P. Van der Meeren, K. Rabaey, High salinity in molasses wastewaters shifts anaerobic digestion to carboxylate production, Water Res. 98 (2016) 293–301.
[40] Z. Zhou, Y. Tao, S. Zhang, Y. Xiao, F. Meng, D.C. Stuckey, Size-dependent microbial diversity of sub-visible particles in a submerged anaerobic membrane bioreactor (SAnMBR): Implications for membrane fouling, Water Res. 159 (2019) 20–29.
[41] J. Chen, M. Zhang, A. Wang, H. Lin, H. Hong, X. Lu, Osmotic pressure effect on membrane fouling in a submerged anaerobic membrane bioreactor and its experimental verification, Bioresour. Technol. 125 (2012) 97–101.
[42] A. Yurtsever, B. Calimlioglu, M. Görür, Ö. Çınar, E. Sahinkaya, Effect of NaCl concentration on the performance of sequential anaerobic and aerobic membrane bioreactors treating textile wastewater, Chem. Eng. J. 287 (2016) 456–465.
[43] L.N. Lemos, R.R. Fulthorpe, E.W. Triplett, L.F.W. Roesch, Rethinking microbial diversity analysis in the high throughput sequencing era, J. Microbiol. Methods 86 (2011) 42–51.
[44] E. Santillan, H. Seshan, F. Constancias, D.I. Drautz-Moses, S. Wuertz, Frequency of disturbance alters diversity, function, and underlying assembly mechanisms of complex bacterial communities, NPJ Biofilms Microbiomes 5 (2019) 8.
[45] J.-G. Na, M.-K. Lee, Y.-M. Yun, C. Moon, M.-S. Kim, D.-H. Kim, Microbial community analysis of anaerobic granules in phenol-degrading UASB by next generation sequencing, Biochem. Eng. J. 112 (2016) 241–248.
[46] S. Wang, X. Hou, H. Su, Exploration of the relationship between biogas production and microbial community under high salinity conditions, Sci. Rep. 7 (2017) 1149.